Evolution of Fe magnetic order in NdFe$_x$Ga$_{1-x}$O$_3$

María Parra-Borderías,[*] Fernando Bartolomé, José
Alberto Rodríguez Velamazán, and Juan Bartolomé

Instituto de Ciencia de Materiales de Aragón and

Departamento de Física de la Materia Condensada,

Universidad de Zaragoza - CSIC, Pedro Cerbuna 12, 50009 Zaragoza, Spain

(Dated: May 18, 2010)

The evolution of the crystal structure and magnetic properties with Fe content in NdFe$_x$Ga$_{1-x}$O$_3$ has been studied by magnetization, ac-susceptibility, x-ray and neutron scattering techniques for $x \geq 0.2$ in order to determine the phase diagram of the series. X-ray diffraction shows that the crystallographic structure of NdFe$_x$Ga$_{1-x}$O$_3$ can be described in the space group *Pbnm* for all x values. Both magnetic ordering and spin reorientation temperatures of the Fe magnetic sublattice decrease with iron concentration due to the presence of Ga magnetic vacancies. The long-range Fe magnetic ordering disappears for $x \leq 0.3$, while ac-susceptibility measurements evidence the presence of short-range Fe ordered clusters and superspin-glass-like effects for x well below the percolation threshold. The complete magnetic structure of the series, including the spin reorientation temperature range is determined by high resolution neutron diffraction analysis. Although the presence of *finite magnetic clusters* for x values close to percolation is evidenced, the study of a percolation quantum phase transition in this series is difficulted by the presence of Nd magnetic moments and a sizeable distribution Δx around the nominal value.

I. INTRODUCTION

Rare-earth oxide compounds with perovskite structure (RMO_3) have been widely studied in solid-state physics due to its rather simple structure and the rich variety of electronic and magnetic phenomena observed, such as magnetoresistance[1] and superconductivity[2,3]. In rare earth (R) and transition metal (M) perovskites both components order in two interspersed simple cubic sublattices that determines the magnetic properties of the sample through the three present magnetic interactions[4]. In general, these interactions follow the hierarchy of M-M, M-R and R-R in descending strength.

Nd orthorhombic perovskites RMO_3 are particularly attractive because of the great number of magnetic and non-magnetic metal ions (M) that can be substituted while maintaining the same structure; an orthorhombically distorted perovskite with four formula units per elementary cell and space group $D_{2h}^{16} - Pbnm$[5,6]. For non-magnetic M ions as Ga, only the collective antiferromagnetic ordering of Nd at $T = 0.97$ K is present[7] due to Nd-Nd exchange interaction. When M is a $3d$ magnetic ion as Fe, Ni or Cr, the M sublattice orders antiferromagnetically with a small canting angle at high temperature T_{N1} due to M-M interaction. T_{N1} ranges from $\sim$700 K for $NdFeO_3$[8] to $\sim$200 K for $NdCrO_3$[9] and $NdNiO_3$[10]. Below T_{N1} the anisotropic M-Nd exchange induces spin reorientation transitions of the M sublattice. In many cases, the antiferromagnetic ordering of M sublattice does not imply a full compensation of the M magnetic moments due to a weak ferromagnetic component. A combination of isotropic and anisotropic M-Nd exchange interactions originated by the weak ferromagnetic and the antiferromagnetic M order, respectively, creates an effective field on the Nd site, H_{M-Nd}. This effective field polarizes the Nd^{3+} spins by splitting the Nd ground state, thus reducing the magnetic entropy available for cooperative Nd-Nd ordering at low temperatures. This Nd polarization has been observed in powder neutron diffraction experiments at low temperatures[11,12]. Depending on the strength of this H_{M-Nd}, cooperative order of Nd sublattice appears at a similar temperature, as in the case where M is a non magnetic metal, f.e. in $NdFeO_3$[13] or $NdNiO_3$[14], whereas it is fully inhibited in others such as in $NdCrO_3$[15] or $NdMnO_3$[16]. It is interesting to note that $NdCrO_3$, the only member of the family in which the low-temperature M magnetic structure is purely antiferromagnetic, is the one with the largest energy splitting of the Nd ground doublet[9,15]: $\Delta/k_B = 27$K.

Another source of rich phenomenology in magnetic orthorhombic perovskites is the intro-

duction of magnetic vacancies in the M sublattice by substitution with a non-magnetic M'
ion. The effects of the dilution are not negligible even for a small concentration of vacancies
and its relevance depends on the nature of the rare-earth ion. In $DyFe_xAl_{1-x}O_3$ the Morin
phase transition temperature increases[17], in $TbFe_xAl_{1-x}O_3$ the reorientation transition tem-
perature decreases[18] while the Tb long-range is inhibited. The same last effect is observed in
$NdFe_xCo_{1-x}O_3$[19], where Co is in a low-spin state. Even in $HoFe_xAl_{1-x}O_3$ a new transition
to a Γ_1 magnetic structure is induced by vacancies[20].

In this paper we consider the case M = Fe, with the substitution of Fe ions by non-
magnetic Ga ions to form the $NdFe_xGa_{1-x}O_3$ series. Each Ga atom is equivalent to the
introduction of a magnetic vacancy in the Fe sublattice. In this case, the nearly complete
antiferromagnetic compensation is destroyed around the neighboring Nd^{3+} ions and a large,
extra isotropic exchange field acting on both R and Fe sublattices arises. We study the effect
of magnetic vacancies on the magnetic ordering of the Fe sublattice and in the polarization of
the Nd sublattice in $NdFe_xGa_{1-x}O_3$. The motivation to use Ga instead of Co as diamagnetic
ion is; besides it has a similar ionic radius to Fe (76 and 78.5 pm respectively), to avoid
deviations of the actual x value from the nominal one. While Ga^{3+} is always diamagnetic,
Co^{3+} ion may change its spin configuration from low- to high-spin depending on neighboring
defects, oxygen vacancies, etc., making difficult to control the paramagnetic fraction in the
high x side.

Diluted magnetic lattices are physical realizations of the magnetic percolation problem.
As the Fe concentration x diminishes, T_{N1} decreases continuously until the percolation
threshold $x = x_c$ is reached, at which $T_{N1} = 0$. In general, x_c depends on the lattice and spin
dimensionality and the sign of the magnetic interaction (ferro- or antiferromagnetic). In our
case, the Fe subsystem can be treated as a Heisenberg antiferromagnetic simple cubic lattice
of $S = 5/2$ spins. There have been both experimental studies and theoretical predictions
for this model. Although early theoretical predictions give a value of $x_c = 0.21$[21], exper-
imental studies on the $S = 5/2$ simple cubic Heisenberg antiferromagnet $KMn_xMg_{1-x}F_3$[22]
find $x_c = 0.31$. This value coincides with the most general value $x_c = 0.31$ predicted for the
percolation problem by Monte Carlo simulations[23,24]. The Fe concentrations near x_c are par-
ticularly interesting. Below x_c, the magnetism of finite clusters may dominate the behavior
of the system, behaving as a distribution of paramagnetic entities with different sizes and
uncompensated moments. In contrast, above x_c the infinite cluster would have regions with

large, uncompensated moments[22]. Moreover, the possibility of a quantum phase transition has been predicted for diluted magnets for x values close to percolation[25,26]. Following previous results on $La_{2/3}Ca_{1/3}Mn_{1-x}Ga_xO_3$ manganites, where a quantum critical point (QCP) associated to the metal-insulating transition induced by Ga doping has been theoretically predicted[27] and claimed experimentally[28], it would be interesting to explore the possibility of a quantum phase transition in $NdFe_xGa_{1-x}O_3$. The posible QCP would be a second-order phase transition occurring at the percolation limit and zero temperature.

The paper is organized as follows; in section II we describe the synthesis and characterization of the samples, and the different experimental techniques. The experimental results will be presented in section III. In subsection III A we analyze the crystallographical structure of the $NdFe_xGa_{1-x}O_3$ compounds. In subsection III B we study the macroscopic magnetic properties of these compounds, while in subsection III C we focus on the complete determination of the magnetic structure of our samples in a wide range of temperatures. Finally, in section IV we summarize the main results obtained.

II.   EXPERIMENTAL DETAILS

$NdFe_xGa_{1-x}O_3$ powder samples were obtained by a standard ceramic route. A stoichiometric mixture of the binary oxides was calcined in air in three consecutive steps of 20h. at 1000°C, 60h. at 1200°C and 80h. at 1400°C, respectively, with intermediate grinding and pressing into pellets the resulting material. Samples $x=0.4$ and $x=0.5$ were subjected to an extra step of 48h at 1400°C, to ensure proper homogeneity throughout the samples close to percolation ($x_c \approx 0.31$). X-ray diffraction analysis was performed on powdered samples to check their quality, showing that all samples are single phase within the accuracy of the technique. Magnetization measurements from 5 K to 600 K, and ac-susceptibility measurements, from 5 K to 400 K, were performed in a SQUID Quantum Design magnetometer. The neutron diffraction experiments were performed on the two-axis diffractometer D1B and the high resolution two-axis diffractometer D2B, at the Institut Laue-Langevin in Grenoble. In both cases a standard ILL ^{4}He gas-flow cryostat was used between 1.5 K and room temperature. At D2B the cryostat was coupled to a cryo-oven from room temperature to 540 K.

III.   EXPERIMENTAL RESULTS AND DISCUSSION
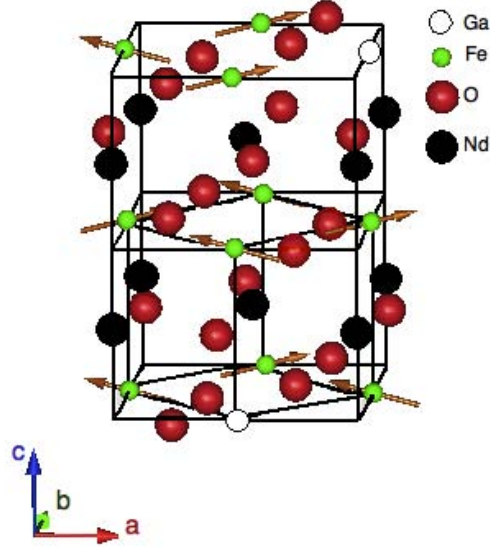
A.   Structure of the samples

Figure 1. Crystallographic and magnetic structure of $NdFe_{0.8}Ga_{0.2}O_3$ at T=94 K.

The crystal structure of $NdFeO_3$ and $NdGaO_3$ is an orthorhombically slightly distorted perovskite described in the space group $Pbnm$[5,29,30], (Z=4). The atoms are located on the following crystallographic sites: Nd^{3+} ions in (4c), Fe^{3+} or Ga^{3+} in (4b) and O^{2-} in (4c) and (8d). Fe^{3+} ions are coordinated by six O^{2-} ions forming FeO_6 octahedra. Therefore the diluted compounds $NdFe_xGa_{1-x}O_3$ are described using the same structure. 4b are special positions and therefore the Fe and/or Ga atoms form a perfect simple cubic (sc) lattice, while the Nd ions are slightly displaced from the ideal sc positions at the middle of the Fe/Ga cubes. A schematic representation of $NdFe_{0.8}Ga_{0.2}O_3$ crystallographic structure is shown in Fig.1 together with its magnetic structure.

X-ray diffraction patterns of the studied compounds show no traces of any impurity phase at the technique sensitivity limit of $\sim 1\%$ in volume. The parameters describing the crystal ordering were refined by the Rietveld method using the FULLPROF program[31,32] and are displayed on Fig. 2. Structural parameters of $NdFeO_3$ and $NdGaO_3$ from Refs 29 and 33

were taken as starting parameters in our analysis. Since gallium ion is slightly smaller (r=76 pm) than the high-spin iron one (r=78.5 pm), the lattice parameter values and the unit cell volume increase with the iron content. No discontinuities are observed in lattice parameters in the whole range of iron concentration and, as expected, all the studied compounds behave as described by the *Pbnm* space group. As can be seen in Fig. 2, our results are in good agreement with previous ones on the non-diluted perovskites and follows Vegard's law. The obtained values of the lattice parameters are displayed in Table I.
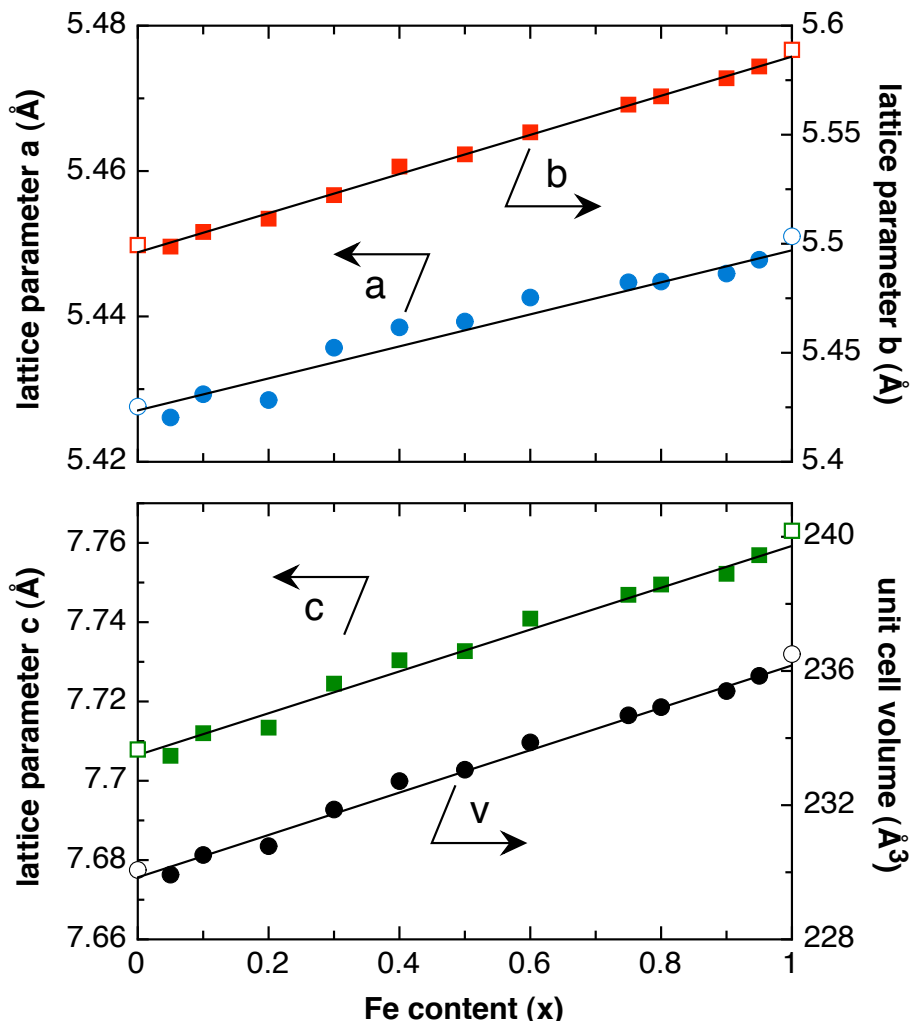

Figure 2. Upper panel: a (●) and b (■) lattice parameters obtained from the Rietveld refinement as a function of iron content. Lower panel: refined c lattice parameter (■) and unit cell volume (●) as a function of iron content. In both panels, lattice parameters of non-diluted compounds from Refs. 29 and 33 are also shown in open symbols.

B. Magnetic analysis

Previous studies on $NdFeO_3$[8,34] showed that, in this structure, iron atoms order magnetically at high temperature (T_{N1} = 690 K) and undergo a spin reorientation transition between T_{SR1} = 190K and T_{SR2} = 80K. Temperature dependent magnetization measured under an applied field of H = 500 Oe of the $NdFe_xGa_{1-x}O_3$ compounds is shown in Fig. 3. T_{N1} decreases with decreasing x due to Fe dilution, and the same holds for T_{SR1} and T_{SR2}. As can be seen in Fig. 3 for some selected examples (x = 0.8, 0.7, 0.6), the same transitions can be observed in $NdFe_xGa_{1-x}O_3$, provided that x values are well above percolation ($x \geq 0.5$). T_{N1} is clearly observed in x = 0.8 and 0.6 as the onset of spontaneous magnetization, due to canted antiferromagnetism as will be shown later by the analysis of neutron diffraction data. The highest temperature reached in the experiment for x = 0.7 was below its T_{N1}, but without any doubt, a similar behaviour as observed in x = 0.8 and 0.6 can be foreseen. On cooling, magnetization shows a clear upturn followed by a strong decrease which coincides with the spin reorientation transition of the Fe magnetic moments. Below $T \sim 40$ K, the magnetization curves for every x show a paramagnetic-like contribution down to the lowest temperatures studied which may be ascribed, at least mainly, to the paramagnetic Nd moments.

The right-bottom panel of Fig. 3 shows the comparison between the magnetization measurements of x = 0.4 and x = 0.3. These two samples are above and below the percolation limit x_c, respectively. The magnetic ordering for x = 0.4 is not clearly observed below 200 K, although a peak that in principle can be identified with the spin reorientation transition is present at T_{SR} = 52 K. The magnetization of x = 0.4 above T = 52 K is rather unexpected, and clearly different from that of a paramagnetic sample, as it is the case for x = 0.3. We have prepared different batches with iron content x = 0.4 (whith longer calcination times and finer intermediate grinding before pressing the material into pellets) with similar results. Evidently, the ceramic route use to prepare the samples does not ensure the exact nominal stoichiometric throughout the whole sample at local scale. Indeed, the magnetization results presented in Fig. 3 suggest the presence of different minority phases with a slightly higher (and also lower) iron content which undergo a continuous appearance of magnetic order. This interpretation is supported by the temperature dependence of neutron diffraction data, as will be presented later.
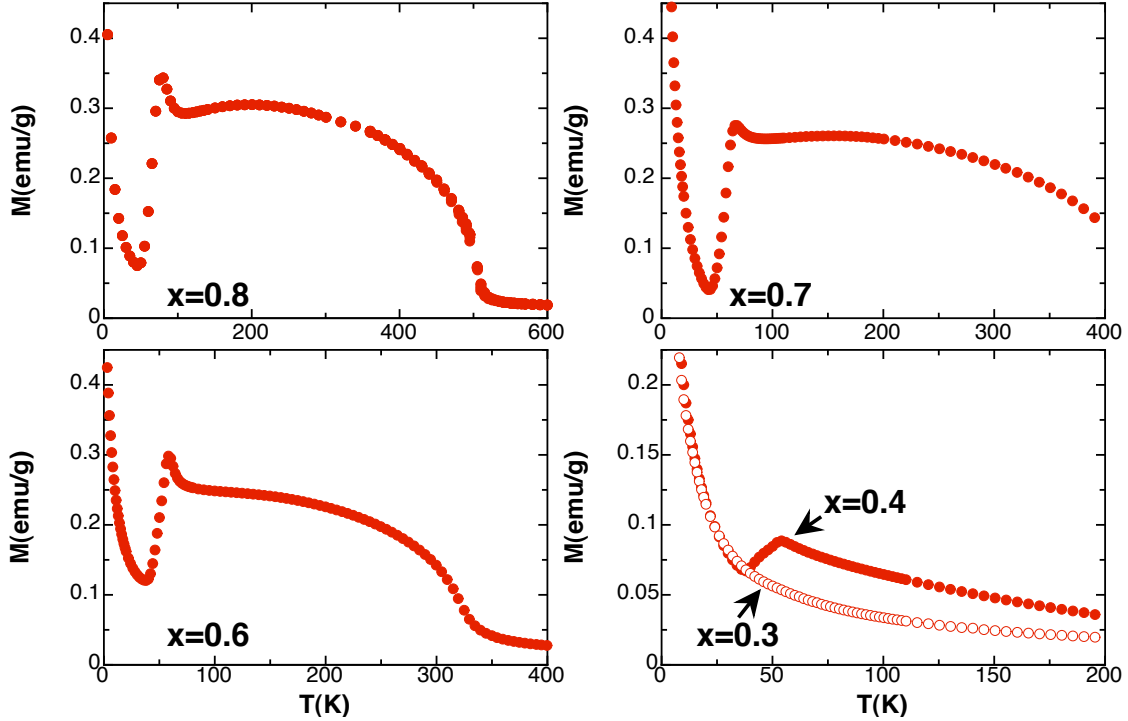
Figure 3. Magnetization as a function of temperature measured at $H = 1000$ Oe of $NdFe_{0}.8Ga_{0.2}O_3$, $NdFe_{0.7}Ga_{0.3}O_3$, $NdFe_{0.6}Ga_{0.4}O_3$, and at $H = 500$ Oe of $NdFe_{0.4}Ga_{0.6}O_3$, and $NdFe_{0.3}Ga_{0.7}O_3$.

Susceptibility measurements on the same samples are displayed in Fig. 4. For samples with iron concentration $x = 0.8$ or higher the observed behavior is similar to the one of $NdFeO_3$[8]. As it is shown in Fig.3, these compounds present a magnetic order transition at high temperature T_{N1} and a spin reorientation process between two lower temperatures T_{SR1} and T_{SR2}. This reorientation process exhibits a double peak in the susceptibility measurement that, in the case of $NdFeO_3$ was assigned to the onset (T_{SR1}) and termination (T_{SR2}) of the reorientation[8]. As the iron concentration decreases the temperature difference between the two peaks ($\Delta T = T_{SR1}$-T_{SR2}) also decreases, being approximatively equal to $\Delta T = 40$ K, 25 K and 20 K for $x = 0.95$, 0.9 and 0.8 respectively. For $x \leq 0.7$ these two peaks merge into one, being the spin reorientation nearly unnoticeable for $x = 0.4$.

For $0.2 \leq x \leq 0.3$, i.e. at $x \lesssim x_c$, the ac-susceptibility measurements at three different excitation frequencies are shown in Fig. 5. Although the real part of χ_{ac} is dominated by the Nd paramagnetic contribution, a small shoulder can be identified near $T = 6$ K and $T = 15$ K for $x = 0.2$ and 0.3 respectively. This shoulder is more clearly shown when subtracting the highest frequency measurement to the other susceptibility curves, as
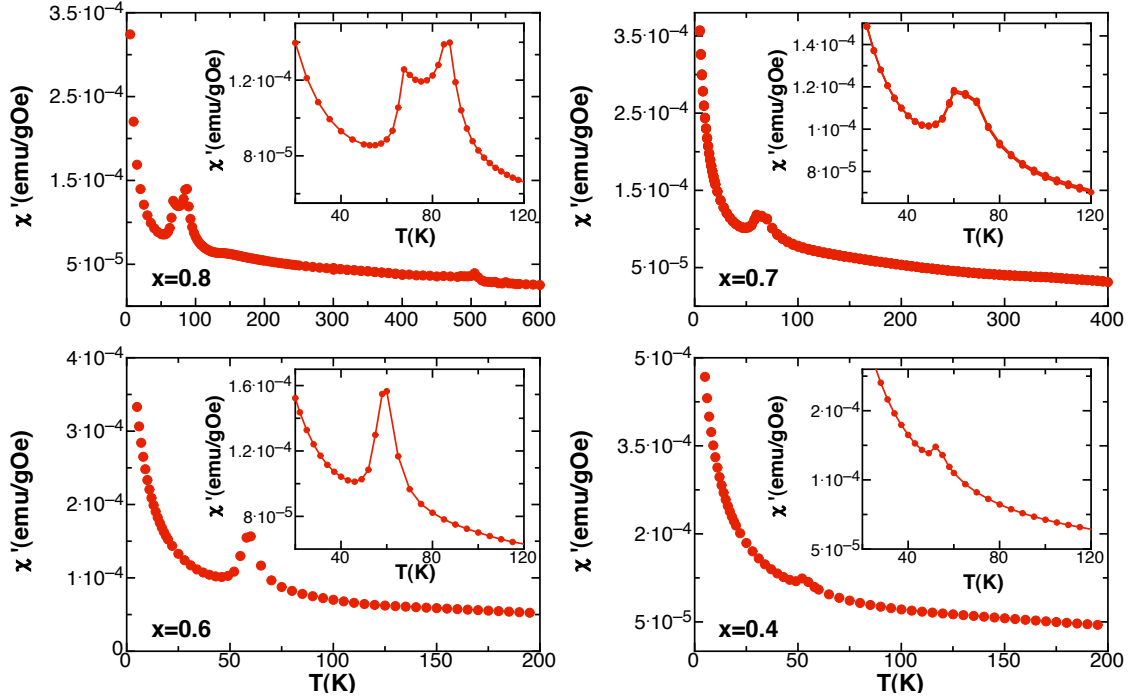
Figure 4. ac magnetic susceptibility as a function of temperature of $NdFe_xGa_{1-x}O_3$, for $x = 0.8$, 0.7, 0.6, and 0.4. The excitation frequency used was 9 Hz.

displayed in Fig. 5 (Right panel). In this figure a maximum at $T \leq 6$ K is present in the real part of χ_{ac} for $x = 0.2$ and two maxima at $T \leq 6$ K and $T \leq 15$ K are evident for $x = 0.3$. The intensity of these maxima decreases as the frequency increases and the temperature at which it appears increases with frequency, resembling the frequency dependence of a spin-glass. As iron concentration for these compounds is below, but close to percolation, we ascribe this cluster-glass-like behavior to the presence of cluster-like regions with slightly higher-than-nominal iron content. These clusters, with a net magnetic moment, may behave as a superparamagnet which is frozen below a certain temperature mainly given by its size. A mainly bimodal distribution of sizes in the $x = 0.3$ sample may originate the χ_{ac} experimental curve. Indeed, the same kind of clusters may be at the origin of the continuous increase in magnetization observed in Fig.3 for $x=0.4$.

The results obtained from magnetic measurements can be summarized in the phase diagram shown in Fig.6. For the sake of clarity, Fig.6 includes information obtained by neutron diffraction, which will be presented in the next section.
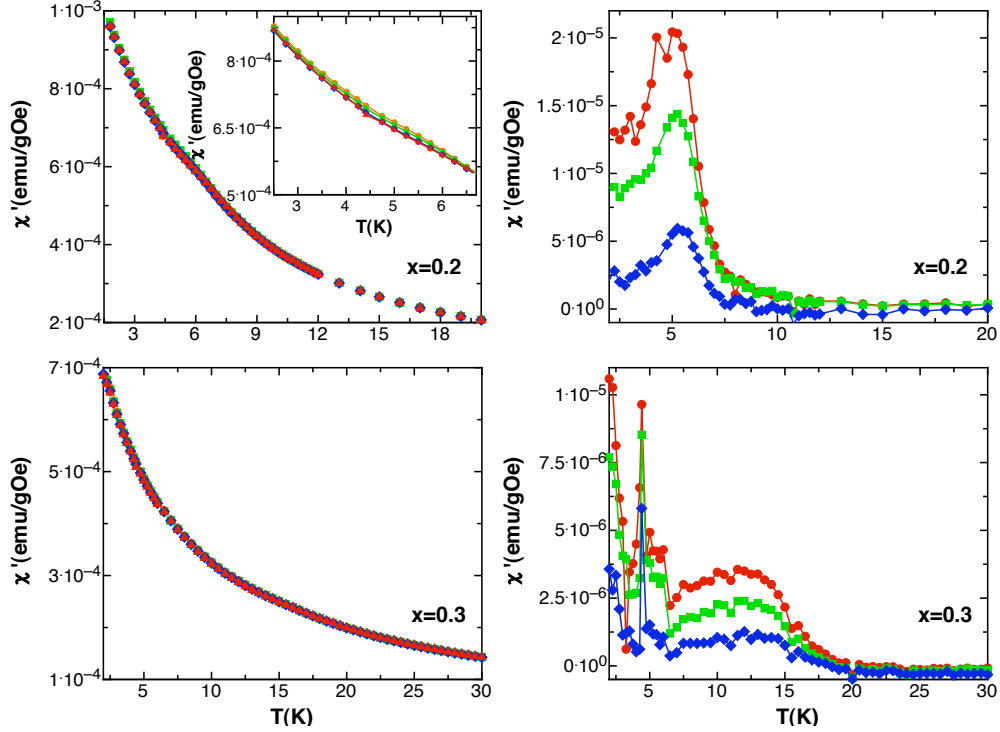
.

Figure 5. (Left column): Real part of the ac-susceptibility as a function of temperature measured at different frequencies on $NdFe_{0.2}Ga_{0.8}O_3$ (upper panel) and $NdFe_{0.3}Ga_{0.7}O_3$ (lower panel). Full circles are χ' values at ν=1.2 Hz, full squares are values at ν=12 Hz, full diamonds are values at ν=120 Hz, and full triangles at ν=1200 Hz. (Right column): χ' as a function of temperature at different frequencies of $NdFe_{0.2}Ga_{0.8}O_3$ and $NdFe_{0.3}Ga_{0.7}O_3$ minus χ' at ν=1200Hz.

C.   Magnetic Structure

In order to determine the magnetic structure of our samples in the range of study shown in Figs. 3 and 4, neutron diffraction experiments were performed. According to previous studies, iron spins in $NdFeO_3$ order correspond to an antiferromagnetic structure with a weak ferromagnetic component G_xF_z (irreducible representation Γ_4)[35]. In the spin reorientation region, marked by the double peak in susceptibility measurements (Fig. 4), the iron spins rotate continuously in the ac plane , from G_xF_z to the low temperature configuration G_zF_x (irreducible representation Γ_2)[36,37]. At low temperatures this configuration induces, via Nd-Fe exchange a Nd polarization of the same symmetry (c_yf_x) that becomes noticeable below $25K$[13]. In our case, the same iron spin configurations are observed for x above percolation, but we have not detected the (100) diffraction peak due to Nd polarization. For $x = 1$, the
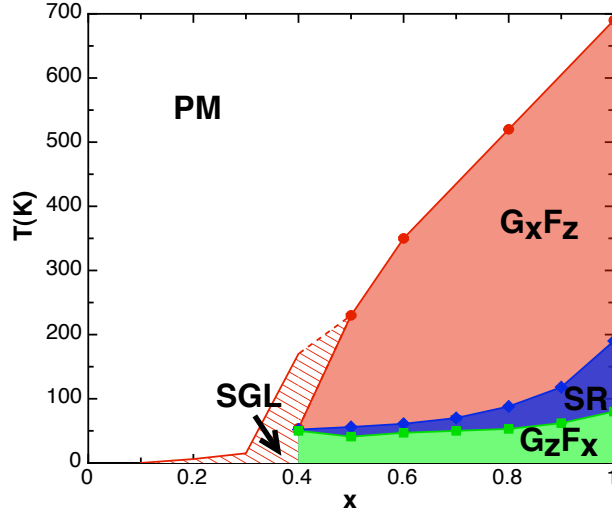
Figure 6. Phase diagram of $NdFe_xGa_{1-x}O_3$ series. The different represented regions are the paramagnetic phase (PM), the Γ_4 high temperature configuration (G_xF_z), the spin reorientation region (SR), the Γ_2 low temperature configuration (G_zF_x) and the cluster-spin-glass phase (SGL). Data of $x=1$ are taken from Ref. 8

isotropic Nd-Fe exchange interaction is nearly cancelled out due to the antiferromagnetic ordering of Fe ions. However, for $x < 1$, an extra isotropic, random exchange field is generated on Nd sites by uncompensated iron spins due to the substitution of some iron by diamagnetic gallium. One would expect this field to be rather strong, due to the nearly compensated antiferromagnetic structure of the Fe lattice in $NdFeO_3$. This random field would polarize the neighbor Nd ion breaking the Γ_2 symmetry, thus preventing the collective antiferromagnetic polarization to be observed. It is worth to mention that for $x = 0.9$ already $\sim 50\%$ of Nd ions are affected by a random field due to some degree of uncompensation of their first Fe neighbors[19].

In Fig. 7 we show, as an example of the analysis, the measured and calculated diffraction patterns obtained at the D2B high-resolution diffractometer of the ILL at $T=38$ K for $NdFe_{0.6}Ga_{0.4}O_3$. The starting structural parameters were taken from our previous x-ray analysis. No significant difference is observed between structural parameters determined by x-ray and neutron diffraction. Since the temperature is lower than the spin reorientation temperature of this compound ($T_{SR}=60$K), the intensity of the diffraction pattern is calculated considering a G_zF_x configuration for the iron spins.

An example of the crystallographic and magnetic structure obtained from the neutron
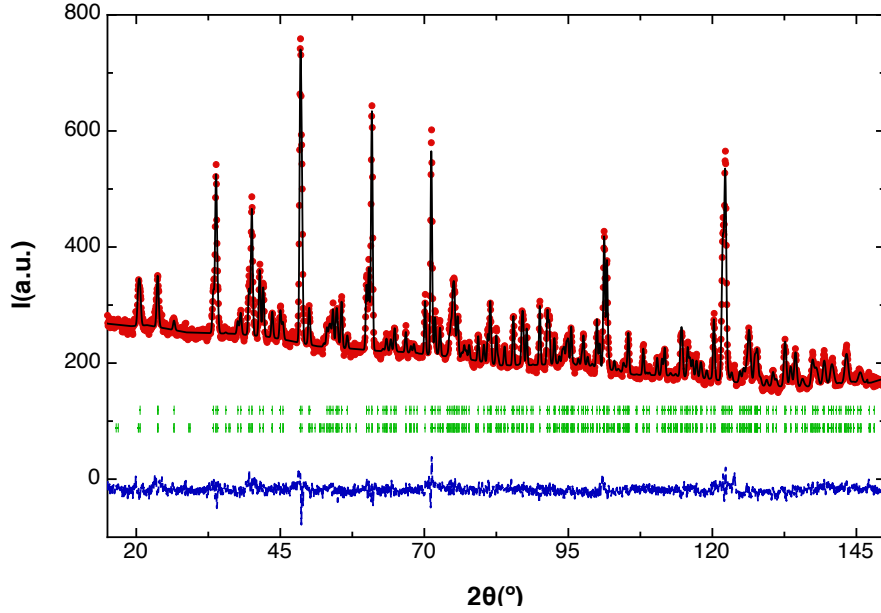
Figure 7. Neutron diffraction pattern of $NdFe_{0.6}Ga_{0.4}O_3$ at $T=38$ K. Full circles shows the observed intensity, solid line shows the calculated intensity, bars shows allowed Bragg reflections for the structural phase (up) and the magnetic phase (down) and dotted line (bottom) shows the difference between the observed and the calculated intensities.

diffraction analysis using FullProf Studio tool[32] is shown in Fig.1. For $NdFe_{0.8}Ga_{0.2}O_3$ and $T=94$K the magnetic configuration of iron spins displays an antiferromagnetic structure along the a axis and a weak ferromagnetic component along the c axis (G_xF_z). In Fig. 8 the diffraction peaks due to iron magnetic ordering obtained at the ILL-D1B diffractometer are displayed. The upper panel shows the (011) and (101) reflections for different iron concentrations at temperatures above T_{SRT}. The intensity of (101) and (011) peaks strongly diminishes as the iron concentration decreases, resulting the first one almost indistinguishable from the corresponding structural peak for $x = 0.4$. This evolution holds for all studied temperatures. As expected, the intensities of the (101) and (011) reflections change strongly from above T_{SR1} and below T_{SR2}. In the reorientation region $T_{SR2} < T < T_{SR1}$ the iron spin rotates continuously from the high temperature structure to the low temperature one and, therefore, it is not possible to fit these reflections with the spin configurations corresponding to either Γ_4 or Γ_2 representations.

The rotation of the four iron magnetic moments present on a unit cell is graphically presented in Fig. 9. The results of the Rietveld refinement for the magnetic moment of the
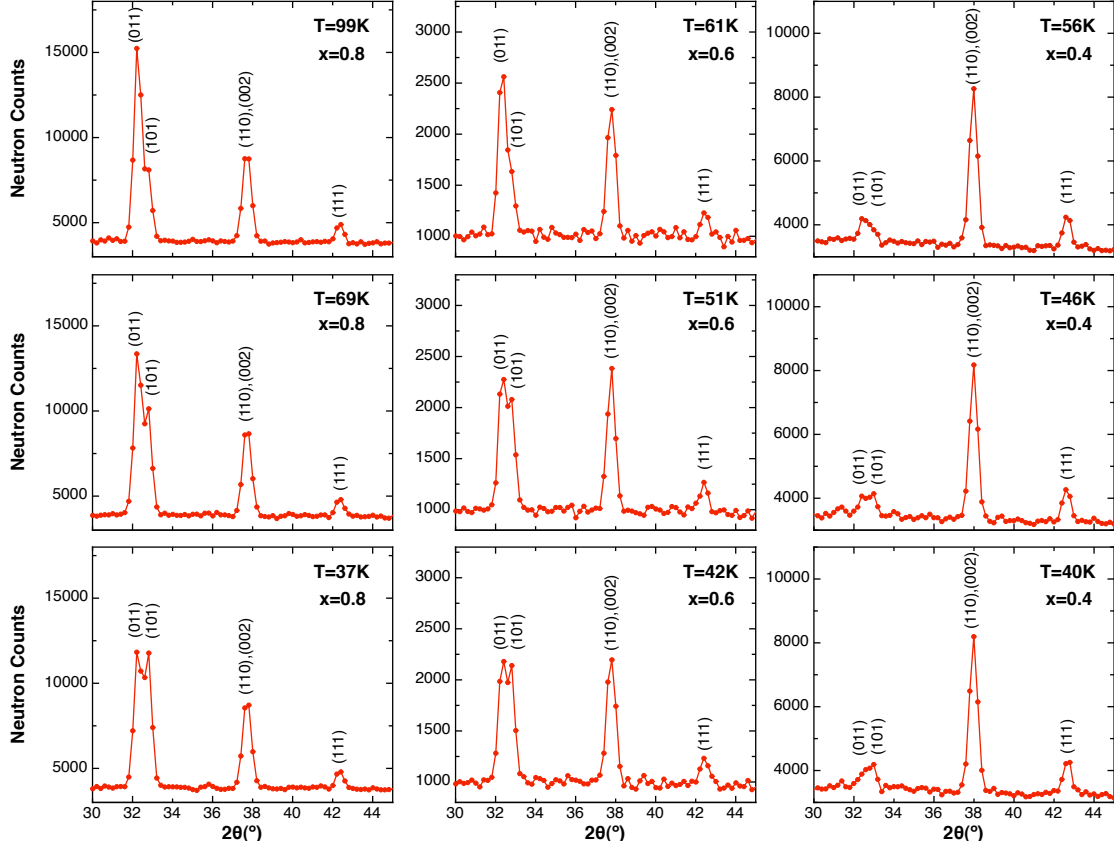
Figure 8. Neutron diffraction patterns for (left panels): $NdFe_{0.8}Ga_{0.2}O_3$, (center panels): $NdFe_{0.6}Ga_{0.4}O_3$, and (right panels): $NdFe_{0.4}Ga_{0.6}O_3$ at three different temperatures; (upper panels):$T > T_{SR1}$; (center panels): $T_{SR1} > T > T_{SR2}$ and (lower panels): $T < T_{SR2}$.

ordered Fe^{3+}ions are shown in Fig. 10

Although some works suggested that the ferromagnetic component is too small to give a measurable contribution to the neutron powder diffraction patterns in $NdFeO_3$[38], several authors have shown that a pure G_x or G_z mode can not explain the ratio between the obtained intensity of (011) and (101) reflections in this material[35,37], both above and below the spin reorientation transition. Moreover, the magnetization measurements show a non negligible magnetization signal, easily observed in a SQUID magnetometer for $0.5 < x < 1$, as shown in Fig. 3. Therefore we performed our Rietveld refinement assuming a $G_x F_z$ ordering for $T>T_{SR}$ and $G_z F_x$ for $T<T_{SR}$. In the spin reorientation region the magnetic moment was allowed to rotate between both configurations by using polar coordinates in the refinement. Neutron powder diffraction measurements do not allow to discriminate between the spin rotation of a single phase and a "phase coexistance model" in which a $G_z F_x$ phase
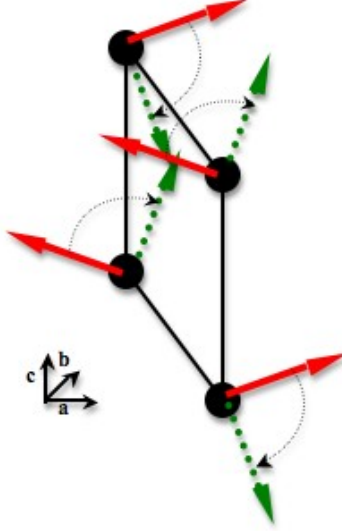
Figure 9. Spin reorientation of iron magnetic moments. Solid line arrows shows magnetic moments orientation at high temperature phase (Γ_4) and dotted line arrows the magnetic moments orientation at low temperature phase (Γ_2)

grows at the expenses of the $G_x F_z$ one. Therefore our results can not be distinguished in principle from those obtained for $NdFeO_3$ in Refs. 39 and 38, where the refinement of neutron powder diffraction patterns of $NdFeO_3$ is performed assuming a $G_x G_z$ ordering in all the temperature range. Although the results are undistinguishable our treatment has the formal advantage of being compatible with the symmetry of the system along the whole temperature range.

Fig. 10 shows the values of the magnetic moment per Fe^{3+} atom resulting from our Rietveld analysis (upper panel), the staggered magnetizations M_x and M_z with the signs corresponding to the iron atom occupying the $(1/2, 0, 0)$ position (central panel) and the angle θ formed by the iron spin at position $(1/2, 0, 0)$ with the z axis as a function of temperature (lower panel) for the samples $x = 0.9$ (left panels), $x = 0.8$ (center panels), and $x = 0.6$ (right panels). The thermal evolution of θ shows a continuous spin reorientation process for $x \geq 0.6$ as observed in the non diluted $x=1$ compound[38,39]. Moreover, no discontinuities in the total magnetic moment are observed during the spin reorientation transition.

As it was already shown in Fig.4, the temperature range at which the spin reorientation occurs decreases as the iron concentration diminishes. According to reference 8, the onset
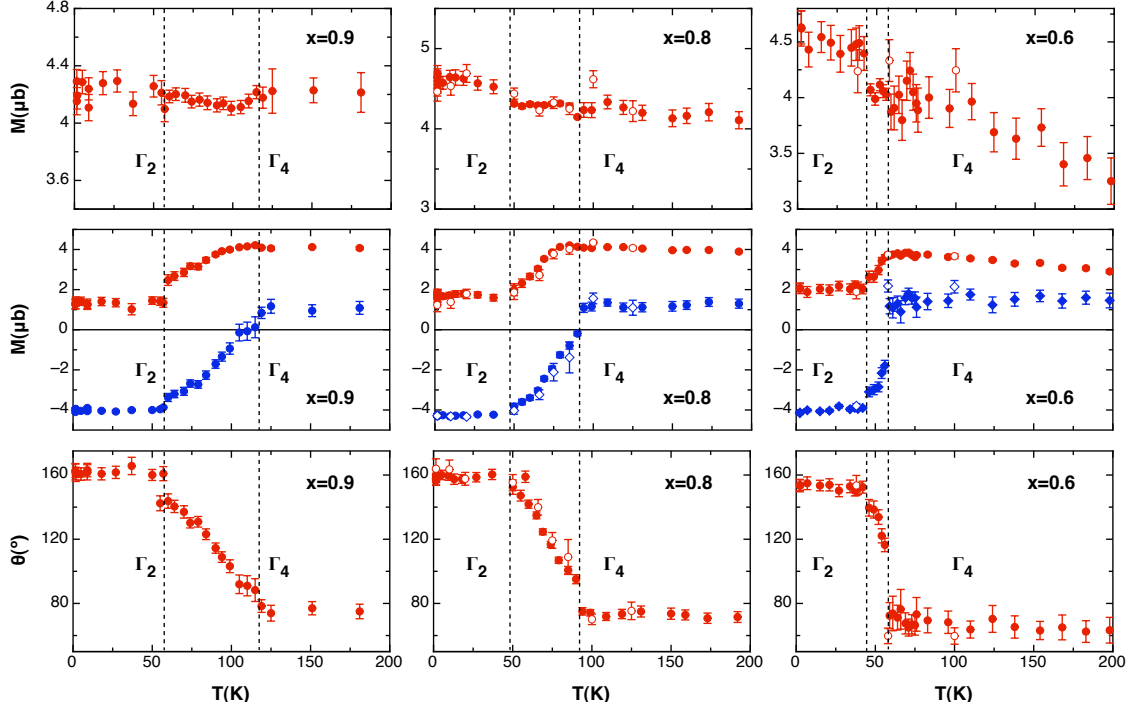
Figure 10. (Upper panel): magnetic moment per Fe^{3+} atom obtained from the Rietveld fit. (Central panel): Absolute values of magnetic moment components per iron atom. Circles correspond to M_x component and diamonds to M_z. (Lower panel) Obtained values of the angle between magnetic moments and c axis. Full symbols are results obtained from measurements performed at the D1B diffractometer while empty symbols correspond to the high-resolution D2B diffractometer.

and termination of the spin reorientation process were associated with a double peak in the susceptibility measurements that is no longer detected in our experiment for $x \leq 0.6$. However, neutron diffraction on the $x = 0.6$ sample shows that the spin reorientation process is not that sharp, although the temperature range is only 14 K wide (see Figs.8 and 10). Since the high temperature peak in the susceptibility curve is higher and wider than the low-temperature one, for low x values the spin reorientation region gets too narrow to distinguish T_{SR1} and T_{SR2} in a χ_{ac} measurement.

The effect of the substitution of Fe by a non magnetic ion in spin reorientation processes has been studied in different rare-earth orthoferrites, as mentioned in Section I, showing that a small concentration of non magnetic ions has an important effect on the magnetic properties of these compounds. The presence of a magnetic vacancy destroys the compensation of the $R - Fe$ isotropic exchange interaction, generating an isotropic exchange field that creates

an additional anisotropy.

In a non-diluted RMO_3 system the isotropic exchange interaction $R - M$ plays no role in the SR process, since the effective field acting on M^{3+} spins due to R^{3+} ions is along the weak ferromagnetic moment. The antisymmetric exchange and the anistropic-symmetric exchange interactions tend to make the M^{3+} and the R^{3+} subsystems perpendicular to each other, generating and effective field on the M^{3+} spins in the direction perpendicular to that of the G_x component:$+H_z$ for up-spins and $-H_z$ for down-spins, that tends to rotate the spins, keeping the antiferromagnetic configuration. As the temperature is lowered, this effective field increases due to R^{3+} moment enhancement. When the interaction created by this field on M^{3+} becomes larger than the anisotropy energy of the metal ions, the spin reorientation transition takes place[40]. In $NdFe_xGa_{1-x}O_3$, as in $TbFe_xAl_{1-x}O_3$[18], the presence of magnetic vacancies increases the Fe ion anisotropy, thus stabilizing the Γ_4 configuration and lowering the temperature at which the spin reorientation transition starts.

The magnitude of the total magnetic moment of Fe^{3+} well above percolation ($x \geq 0.6$), both above and below the spin reorientation process, is in good agreement with previous neutron powder diffraction studies on $NdFeO_3$[34,37–39,41], and so are the values of the canting angles. All these data, together with the spin reorientation process data and magnetic ordering of Fe spins are given in Table I. It is interesting to note that the canting angle, both above and below the reorientation transition increases with the gallium concentration. The antiferromagnetic component of iron moments becomes uncompensated by substituting iron atoms by gallium. Therefore, the average strength of the exchange interaction decreases and iron spins might rotate slightly, decreasing the effective magnetic moment in the G mode. This effect is specially remarkable for $x = 0.4$, where the canting angle is increased by a factor of three with respect to that of $NdFeO_3$, as can be seen in Table I. Moreover, in $x = 0.4$ the magnetic moment per Fe obtained from the Rietveld refinement is only $\sim 2.4\mu_B$ in comparison with $\sim 4.2\mu_B$ for $x = 0.9$. This may indicate that only a half of the iron spins in the $x = 0.4$ sample are ordered, consistently with the scenario suggested by the magnetization measurements on this sample shown in Fig. 3: in $NdFe_{0.4}Ga_{0.6}O_3$ iron atoms are not equally distributed through the sample, with Fe-rich and Fe-poor regions in which iron concentration vary. Iron atoms in Fe-poor regions, where effective x is below percolation, would not be ordered, and, therefore, would not contribute to the measured intensity of the G and F modes.
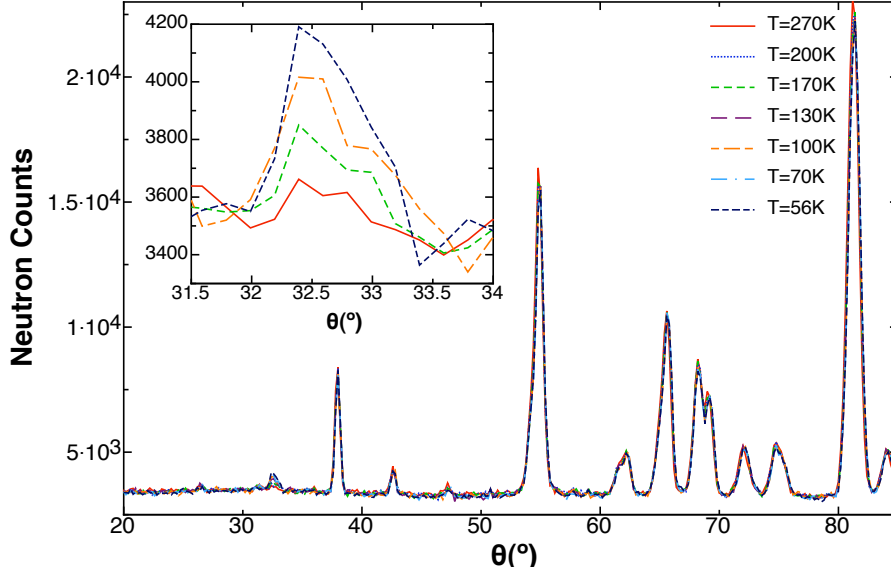
Figure 11. Neutron diffraction patterns of NdFe$_{0.4}$Ga$_{0.6}$O$_3$ at different temperatures, above spin reorientation. Inset shows a zoom on the (0 1 1) (1 0 1) peaks for some selected temperatures.

The experimental evidence of this different concentration regions is shown in Fig. 11. The neutron diffraction pattern of the $x = 0.4$ sample shows a continuous increase with temperature of the (1 0 0) and (1 0 1) peaks, while in magnetization and susceptibility measurements displayed in Figs. 3 and 4 no order transition is observed, besides the spin reorientation process. Note that $T_{SR1}^{x=0.4} \approx 52$ K is lower than the temperatures at which the diffraction patterns in Fig. 11 have been recorded. However, magnetization measurements did not allow to identify the ordering temperature above $T_{SR1}^{x=0.4}$. The continuous enhancement of the (1 0 0) and (1 0 1) peaks in a wide range of temperatures (from $\sim$200 K) starts at temperatures close to the magnetic order of NdFe$_{0.5}$Ga$_{0.5}$O$_3$. The magnetization measurement also shows the continuous appeareance of a net magnetic moment above the paramagnetic background below $T = 200$ K. These results suggest that, even for crystallographically monophasic samples, one can not avoid a certain chemical distribution, that originates regions with Fe concentrations slightly different from the nominal one. Usually the effect of these small regions is not predominant, since the effect of the majority phase dominates the system, specially below its ordernig transition. However, for iron concentrations close to percolation, the effect of these Fe-rich regions is no longer negligible since no ordering effect takes place. Our results suggest that intrinsical disorder, leading to clus-

terization of the sample is always present, for concentrations close to percolation with the ceramic fabrication route described in section II.The small fraction of the sample with iron concentration slightly different from the nominal one can be minimized by repeating the sinterization process, but it appears to be always present in our samples. The relaxation processes taking place at different low temperatures in the $x = 0.3$ sample is consistent with the presence of Fe clusters with a distribution of sizes, or magnetic "*rare regions*", as coined by Vojta in Ref. 42.

One may wonder whether Fe in $NdFe_xGa_{1-x}O_3$ is an aproppriate scenario to test quantum phase transitions at concentrations close to percolation, as suggested by Vojta[42]. Two problems arise in this system to compare experimental results with theoretical predictions. First, the presence of paramagnetic Nd in the background makes extremely difficult to obtain critical exponents from magnetic susceptibility measurements in samples near $x = 0.312$[22–24], as evidenced in Figs. 3 and 4. Second, the percolative quantum phase diagram suggested by Vojta[26,42] indicates that the effect of quantum fluctuations would be a higher than expected critical temperature for concentrations near (and higher than) percolation. This may appear to be the case in $NdFe_{0.4}Ga_{0.6}O_3$ as magnetization and neutron diffraction experiments show. However, the experimental results may be simply due to the ordering of a wide distribution of Fe-rich regions, with higher than nominal concentrations and therefore, higher than expected critical temperatures. Evidently, this *"compositional distribution"* makes difficult the study of quantum phase transitions at concentrations close to percolation. The use of non-magnetic rare earth, like in the $LaFe_xGa_{1-x}O_3$ series, may pave the way to future (quantum) critical exponents search.

IV. CONCLUSIONS

In this work we have shown that Fe ions in $NdFexGa_{1-x}O_3$ compounds order magnetically for $x \geq 0.4$ in the same configuration observed in $NdFeO_3$, Γ_4, but at a lower temperature due to Fe dilution. The Fe ion anisotropy increment due to the substitution of Fe by a non magnetic metal depresses the spin reorientation temperature of the metal sublattice. However, the effect is not as large as described in other systems as $TbFe_{1-x}Al_xO_3$[18], in which the spin reorientation process is fully inhibited by a 2.5% aluminum concentration due to the strong Ising character of the Tb ion. The lowest doublet of the Nd^{3+} in $NdGaO_3$

Table I. a, b, and c lattice parameters at room temperature, temperature at which the spin reorientation begins, temperature of spin reorientation termination,ΔT_{SR}, T_C, canted angle at $T>T_{SR}$, canted angle at T=1.5K, $|\mu_{Fe}|$ at $T>T_{SR}$ and at T=1.5K of all compounds analysed in this work. Data of NdFeO$_3$ from Refs. 8,37,and 38 are also shown.

	a	b	c	T_{SR1}(K)	T_{SR2}(K)	ΔT_{SR}(K)	T_C(K)	θ_1(°)	θ_2(°)	$\|\mu_{Fe}\|_1(\mu_B)$	$\|\mu_{Fe}\|_2(\mu_B)$
Ref.38 - NdFeO$_3$	5.451 02	5.588 08	7.761 65	190	100	90	-	13	20	3.87(5)	4.18(5)
Ref.8 - NdFeO$_3$	-	-	-	190	80	110	690	-	-	-	-
Ref.37 - NdFeO$_3$	-	-	-	-	-	-	-	-	20.6	-	4.12(5)
NdFe$_{0.9}$Ga$_{0.1}$O$_3$	5.4459	5.5759	7.7522	118±1	62.0±1	56±1.4	-	13±4	18±5	4.22±0.14	4.16±0.1
NdFe$_{0.8}$Ga$_{0.2}$O$_3$	5.4448	5.5676	7.7495	88±1	53±0.5	35.0±1.1	520±1	19±3	22±3	4.1±0.05	4.46±0.12
NdFe$_{0.7}$Ga$_{0.3}$O$_3$	-	-	-	70±3	50±1	20±3	-	-	-	-	-
NdFe$_{0.6}$Ga$_{0.4}$O$_3$	5.4426	5.511	7.7409	61±1	47±1	14.0±1.4	350±2	21±8	26±3	4.00±0.18	4.62±0.14
NdFe$_{0.5}$Ga$_{0.5}$O$_3$	5.4393	5.541	7.7327	56±1	51±1	4.0±1.4	230±2	-	-	-	-
NdFe$_{0.4}$Ga$_{0.6}$O$_3$	5.4385	5.5354	7.7304	52±1	50±1	2.0±1.4	54±2	37±12	31±9	2.42±0.13	2.74±0.22

has been proved to be slightly Ising-like[43]. However, the high temperatures at wich the spin reorientation takes place in NdFeO$_3$ ensures the thermal population of several crystal field doublets of the Nd ion[7], reducing even more the weight of its Ising ground doublet. Therefore, the Fe spin reorientation is not inhibited even for Ga concentrations as high as 60%. The reduction of T_{SR1} and T_{SR2} is found to narrow the reorientation temperature range, being nearly negligible for $x = 0.4$, for which a sharp Γ_4-Γ_2 transition is observed in less than $\Delta T = 2$ K. These results are summarized in Table I and in Fig.6

The uncompensated isotropic exchange field generated by the magnetic vacancies on Nd sites magnetize Nd ions along $G_z F_x$ for $T<T_{SR}$, therefore even at the higher Fe concentrations no peak due to Nd polarization is observed in neutron diffraction measurements. Magnetic vacancies induce an increment in the canted angle of the Fe spins both in the high- (Γ_4) and in the low-temperature (Γ_2) phases. However, for Fe concentrations well above percolation these canted angle values are in good agreement with previous results on NdFeO$_3$ and so are the Fe magnetic moments, ensuring that magnetic vacancies do not influence the ordering type found for Fe in the diluted phase.

Indeed, for $x = 0.4$, our fits to neutron diffraction data indicate that the ordered magnetic moment per Fe ion is $2.4\mu_B$, which amounts only to 60% of the value for the pure $NdFeO_3$, pointing along a canting angle which is almost twice that found in the pure compound. Moreover, no Néel temperature is clearly observed on the $x = 0.4$ sample, and the ordering appears to be distributed below $T = 170\,K$ and $T = 52\,K$, both in magnetization and neutron diffraction experiments. All these facts indicate a strong magnetic disorder in this system. In $x = 0.2$ and 0.3 the magnetic susceptibility data indicate the presence of relaxation processes that may be related with the presence of cluster-glass-like phases. Both samples present a common feature at $T \sim 5$ K, while $x = 0.3$ has another one at $T \sim 12$ K. This suggests the freezing of magnetic moments of Fe clusters of different sizes and momenta, whose concentration obviously depends on x.

Near percolation ($0.2 \leq x \leq 0.4$), three related dilution effects will influence the magnetism of the system. First, above percolation the fractal nature of the infinite cluster[22,44] induces the presence of magnetically uncompensated regions, which are expected to have a paramagnetic behavior, thus reducing the ordered magnetic moment per Fe. Second, both above and below percolation, even in a chemically perfect distribution, the presence of finite clusters is ensured. The random net magnetic moment, interactions and anisotropy of these entities will reduce the ordered magnetic moment per Fe atom, as well as may give raise to glassy behavior. Third, a chemical concentration distribution of Fe and Ga is intrinsically related to the ceramic fabrication route, generating regions with local Fe concentrations higher and lower than nominal, which may induce a distribution of magnetic properties, and in particular, the T_N of the $x = 0.40$ system observed both in macro- and microscopic magnetic measurements.

The random isotropic exchange field created by Fe on the Nd system as a result of Ga dilution inhibits the Nd polarisation in $NdFe_xGa_{1-x}O_3$, as observed in neutron diffraction. The influence of Ga dilution and Fe magnetic disorder on the cooperative ordering of Nd taking place in the pure compounds[7,45] at $T = 1K$ is currently under study.

ACKNOWLEDGMENTS

---

[*] mariapb@unizar.es

[1] H. Y. Hwang, S.-W. Cheong, P. G. Radaelli, M. Marezio, and B. Batlogg, Phys. Rev. Lett. **75**, 914 (Jul 1995).

[2] H.-C. Z. Loye, K. J. Leary, S. W. Keller, W. K. Ham, T. A. Faltens, J. N. Michaels, and A. M. Stacy, Science, New Series **238**, 1558 (1987), ISSN 00368075, http://www.jstor.org/stable/1700976.

[3] S. Kondoh, M. Sera, Y. Ando, and M. Sato, Physica C: Superconductivity **157**, 469 (1989), ISSN 0921-4534, http://www.sciencedirect.com/science/article/B6TVJ-46FR23X-DC/2/d409cfd248cd51de41f507c7ae3968d4.

[4] K. Belov, A. Zvezdin, and A. Kadomtseva, "Soviet scientific reviews. section a. physics reviews," (Harwood Academic Publishers, 1987) Chap. Rare-earth orthoferrites, symmetry and non-Heisenberg exchange, pp. 117–222.

[5] S. Geller and E. Wood, Acta Crystaolgraphica **9**, 563 (1956).

[6] E. Bertaut and F. Forrat, Journal de Physique et Le Radium **17**, 129 (1956).

[7] F. Bartolomé, M. Kuz'min, R. Merino, and J. Bartolomé, IEEE Transactions on magnetics **30**, 960 (March 1994).

[8] R. Hornreich and I. Yaeger, International Journal of Magnetism **4**, 71 (1973).

[9] R. M. Hornreich, Y. Komet, R. Nolan, B. M. Wanklyn, and I. Yaeger, Phys. Rev. B **12**, 5094 (Dec 1975).

[10] J. L. García-Muñoz, J. Rodríguez-Carvajal, and P. Lacorre, Phys. Rev. B **50**, 978 (Jul 1994).

[11] P. Pataud and J. Sivardière, Le journal de physique **31**, 803 (August-Septembre 1970).

[12] I. Sosnowska and P. Fischer, Phase Transitions **8**, 319 (1987).

[13] J. Bartolome, E. Palacios, M. Kuzmin, F. Bartolome, I. Sosnowska, R. Przenioslo, R. Sonntag, and M. Lukina, Physical Review B **55**, 11432 (MAY 1 1997), ISSN 0163-1829.

[14] F. Bartolome, J. Bartolome, and R. S. Eccleston, Journal of Applied Physics **87**, 7052 (2000), http://link.aip.org/link/?JAP/87/7052/1.

[15] F. Bartolome, J. Bartolome, M. Castro, and J. J. Melero, Phys. Rev. B **62**, 1058 (Jul 2000).

[16] F. Bartolome, J. Herrero-Albillos, L. Garcia, J. Bartolome, N. Jaouen, and A. Rogalev, Journal of Applied Physics **97** (MAY 15 2005), ISSN 0021-8979, doi:\bibinfo{doi}{10.1063/1.1850810}, 49th Annual Conference on Magnetism and Magnetic Materials, Jacksonville, FL, NOV 07-11, 2004.

[17] A. Kadomtseva, A. Zvezdin, M. Lukina, V. Milov, A. Mukhin, and T. Ovchinnikova, Zhurnal Eksperimentalnoi I Teoreticheskoi Fizikiz **46**, 1216 (December 1977).

[18] V. Derkachenko, A. Zvezdin, A. Kadomtseva, N. Kovtun, M. Lukina, and A. Mukhin, Physica Status Solidi A-Applied Research **84**, 215 (1984), ISSN 0031-8965.

[19] F. Bartolomé and J. Bartolomé, Solid State Sciences **7**, 700 (April 2005).

[20] A. Zvezdin, A. Kadomtseva, and A. Mukhin, Izvestiya Akademii Nauk SSSR Seriya Fizicheskaya **44**, 1348 (1980), ISSN 0367-6765.

[21] R. J. Elliott and B. R. Heap, Proceedings of the Royal Society of London. Series A, Mathematical and Physical Sciences **265**, 264 (1962), ISSN 00804630, http://www.jstor.org/stable/2414233.

[22] D. Breed, K. Gilijamse, J. Sterkenburg, and A. Miedema, Journal of Applied Physics **41**, 1267 (1970).

[23] A. Sur, J. L. Lebowitz, J. Marro, M. H. Kalos, and S. Kirkpatrick, Journal of Statistical Physics **15**, 345 (1976).

[24] Y. Deng and H. W. J. Blöte, Phys. Rev. E **72**, 016126 (Jul 2005).

[25] S. Sachdev, *Quantum Phase Transitions* (Cambridge University Press, 1999).

[26] T. Vojta and J. Schmalian, Phys. Rev. Lett. **95**, 237206 (Nov 2005).

[27] J. Alonso, L. Fernandez, F. Guinea, V. Laliena, and V. Martin-Mayor, Physical Review B **66** (SEP 1 2002), ISSN 1098-0121, doi:\bibinfo{doi}{10.1103/PhysRevB.66.104430}.

[28] J. De Teresa, P. Algarabel, C. Ritter, J. Blasco, M. Ibarra, L. Morellon, J. Espeso, and J. Gomez-Sal, Physical Review Letters **94** (MAY 27 2005), ISSN 0031-9007, doi:\bibinfo{doi}{10.1103/PhysRevLett.94.207205}.

[29] W. Marti, M. Medarde, S. Rosenkranz, P. Fischer, A. Furrer, and C. Klemenz, Physical Review B **52**, 4275 (AUG 1 1995), ISSN 0163-1829.

[30] M. Marezio, J. Remeika, and P. Dernier, Acta Crystallograhica. Section B **26**, 2008 (1970).

[31] J. Rodriguez-Carvajal, Physica B **192**, 55 (October 1993).

[32] T. Roisnel and J. Rodriguez-Carvajal, in *Proceedings of the Seventh European Powder Diffraction Conference (EPDIC 7)*, edited by R. Delhez and E. Mittenmeijer (2000) pp. 118–123.

[33] L. Vasylechko, L. Akselrud, W. Morgenroth, U. Bismayer, A. Matkovskii, and D. Savytskii, Journal of Alloys and Compounds **297**, 46 (2000).

[34] W. C. Koehler, E. O. Wollan, and M. K. Wilkinson, Physical Review **118**, 58 (Apr 1960).

[35] I. Sosnowska and E. Steichele, AIP Conference Proceedings, 309(1982), ISSN 0094-243X.

[36] K. Belov, A. Kadomtseva, T. Ovchinnikova, V. Timofeeva, and V. Uskov, Soviet Physics- Solid State **13**, 518 (August 1971).

[37] R. Przenioslo, I. Sosnowska, P. Fischer, W. Marti, F. Bartolomé, J. Bartolomé, E. Palacios, and R. Sonntag, Journal of Magnetism and Magnetic Materials **160**, 370 (1996).

[38] W. Slawinski, R. Przeniosko, I. Sosnowska, and E. Suard, Journal of Physics: Condensed Matter, 4605(July 2005).

[39] I. Sosnowska, E. Steichelea, and A. Hewat, Physica B+C **136**, 394 (1986), ISSN 0378-4363, neutron Scattering, Proceedings of the International Conference on Neutron Scattering.

[40] T. Yamaguchi, Journal of Physics and Chemistry of Solids **35**, 479 (1974).

[41] R. Przenioslo, I. Sosnowska, and P. Fischer, Journal of Magnetism and Magnetic Materials **140-144**, 2153 (1995).

[42] T. Vojta, Journal of Physics A: Mathematical and General **39**, R143 (2006), `http://stacks.iop.org/0305-4470/39/i=22/a=R01`.

[43] F. Luis, M. Kuz'min, F. Bartolome, V. Orera, J. Bartolome, M. Artigas, and J. Rubin, Physical Review B **58**, 798 (July 1998).

[44] L. de Jongh, in *Proceedings of the European Physical Society Summer School on Magnetic Phase Transitions, Ettore Majorana Centre, Erice, Italy*, Series in Solid State Sciences, Vol. 48, edited by M. Ausloos and R. J. Elliott (Springer, New York, 1983) p. 172.

[45] F. Bartolome, M. Kuzmin, J. Bartolome, J. Basco, J. Garcia, and F. Sapina, Solid State Communications **91**, 177 (JUL 1994), ISSN 0038-1098.